



HAL
open science

Minuet motion of a pair of capsules interacting in simple shear flow

X.-Q. Hu, X.-C. Lei, Anne-Virginie Salsac, Dominique Barthès-Biesel

► To cite this version:

X.-Q. Hu, X.-C. Lei, Anne-Virginie Salsac, Dominique Barthès-Biesel. Minuet motion of a pair of capsules interacting in simple shear flow. *Journal of Fluid Mechanics*, 2020, 892, pp.A19. 10.1017/jfm.2020.181 . hal-02818230

HAL Id: hal-02818230

<https://utc.hal.science/hal-02818230v1>

Submitted on 6 Jun 2020

HAL is a multi-disciplinary open access archive for the deposit and dissemination of scientific research documents, whether they are published or not. The documents may come from teaching and research institutions in France or abroad, or from public or private research centers.

L'archive ouverte pluridisciplinaire **HAL**, est destinée au dépôt et à la diffusion de documents scientifiques de niveau recherche, publiés ou non, émanant des établissements d'enseignement et de recherche français ou étrangers, des laboratoires publics ou privés.

Minuet motion of a pair of capsules interacting in simple shear flow

X.-Q. Hu^{1,2}, X.-C. Lei², A.-V. Salsac^{1,†} and D. Barthès-Biesel¹

¹Biomechanics and Bioengineering Laboratory (UMR CNRS 7338), Université de Technologie de Compiègne, Alliance Sorbonne Université, CS 60319, 60203 Compiègne, France

²State Key Laboratory of Advanced Design and Manufacturing for Vehicle Body, College of Mechanical and Vehicle Engineering, Hunan University, 410082 Changsha, China

(Received xx; revised xx; accepted xx)

We study the three-dimensional hydrodynamic interaction of a pair of identical, initially spherical capsules freely suspended in a simple shear flow under Stokes flow conditions. The capsules are filled with a Newtonian liquid (same density and viscosity as the suspending fluid). Their membranes satisfy the neo-Hookean constitutive law. We consider the rarely studied case where the capsule centres are initially located in (or near) the plane defined by the flow direction and the vorticity vector, i.e. in two different shear planes. The motion and deformation of the capsules are modelled by means of a boundary integral technique to compute the flows, coupled to a finite element method to calculate the force exerted by the membranes on the fluids. We follow the motion and deformation of the capsules as they are convected towards each other after a sudden start of the flow. Our main finding is that, depending on their initial position and deformability, the two capsules may oscillate slowly about the flow gradient axis, get nearer to each other at each oscillation to finally interact strongly and separate. This minuet motion had not been identified previously. We identify the regions of space where either simple crossing or minuet occur. This phenomenon has a marked influence on the irreversible trajectory drift of two capsules after crossing: the minuet process leads to a significant trajectory displacement along the flow gradient when none was expected, based on the previous studies where the two capsules had a significant relative velocity.

Key words:

1. Introduction

The hydrodynamics of pairwise interaction of deformable particles is a crucial topic for semi-dilute suspension rheology (Batchelor & Green 1972*a*; Guazzelli & Morris 2012). When the particles are deformable, their shear induced deformation leads to non-Newtonian and to self-diffusion effects. This has been demonstrated for liquid droplets (Loewenberg & Hinch 1997; Guido & Simeone 1998). The case of capsules (liquid drop enclosed by a thin elastic membrane) is particularly complex because the motion and deformation of those particles result from non-linear fluid-structure interactions that are difficult to model. For example, the capsules may be highly deformed as they cross each other, which leads to the formation of a thin liquid film between the two particles and to potential damage of the membrane due to high shearing forces.

† Email address for correspondence: anne-virginie.salsac@utc.fr

This phenomenon is usually studied in a simple shear flow $v_1^\infty = \dot{\gamma} x_2, v_2^\infty = v_3^\infty = 0$ in a laboratory Cartesian reference frame, where $\dot{\gamma}$ is the shear rate. The two capsules C_1 and C_2 are initially positioned with distances $\Delta X_1^{(0)}, \Delta X_2^{(0)}, \Delta X_3^{(0)}$ between their centres. The first three-dimensional model of two initially spherical identical capsules (radius a) interacting in simple shear flow is due to Lac *et al.* (2007), who considered the case where the two capsules had their centres in the same $x_1 x_2$ shear plane ($\Delta X_3^{(0)} = 0$). The capsule membrane is treated as a very thin sheet of a hyperelastic material devoid of bending resistance and the flow Reynolds number is assumed to be negligible. Lac *et al.* showed that, in a reference frame centered on C_1 , capsule C_2 is first displaced along the velocity gradient so that it can overpass ('jump over') C_1 and it is then shifted back towards the flow axis as it moves away. However, the final separation $\Delta X_2^{(f)}$ is larger than the initial one $\Delta X_2^{(0)}$. The crossing thus leads to an irreversible trajectory shift along the shear gradient (x_2 -direction). This effect, which decreases with an increase of the capsule deformability and/or the initial distance $\Delta X_2^{(0)}$, ultimately leads to self-diffusion effects in a suspension. We propose to call this crossing process the *leapfrog* motion. The same situation was later considered where the two spherical capsules were replaced by two red blood cells (Omori *et al.* 2013) or two vesicles (Gires *et al.* 2014). In both instances, it is found that the particles do a leapfrog motion with a trajectory shift that evolves qualitatively as found previously by Lac *et al.* Experimental measurements of the trajectory of liquid filled giant lipid vesicles compare well with the predictions of the flow model (Kantsler *et al.* 2008; Gires *et al.* 2014). In all the aforementioned studies, the flow field around the capsules was computed by means of the boundary integral representation of the Stokes equations. As a consequence, the pair of capsules is effectively interacting in an infinite flow domain.

Finite differences and front tracking techniques can also be used to study the interaction problem: this allows to consider non-Newtonian or finite inertia effects in the suspending fluid. The computation is usually performed in a flow domain, bounded by two walls parallel to the $x_1 x_3$ -plane where the velocity is imposed (to create the simple shear flow). On the other boundaries of the box, periodic flow conditions are imposed. Doddi & Bagchi (2008) used this technique to model the pair interaction of two initially spherical capsules, when the inertia of the flow was not negligible. They found that when the flow Reynolds number increased, the capsules did not cross, but reversed their motion. This phenomenon was confirmed for a pair of liquid droplets (Olapade *et al.* 2009). However, the spiraling motion reported by Doddi and Bagchi, is linked to the size of their computational domain and is a confinement effect. Indeed, for the results to be independent of the computational procedure and to be transposable to unbounded flow situations, the domain has to be large enough, typically $40a \times 10a \times 5a$, for in-shear-plane crossing (Olapade *et al.* 2009). Pranay *et al.* (2010) considered the case where the suspending fluid is a dilute polymeric solution. They found that the presence of polymer leads to a decrease of the trajectory shift only when the capsule deformability is low. A recent study (Singh & Sarkar 2015) considered the pair interaction of two capsules with different deformability and found that the trajectory shift is influenced by the stiffness ratio. All the studies based on finite difference and front tracking techniques only considered pairs of capsules with their centroids in the same shear plane, where they remain because of the problem symmetry.

However, in a suspension, two nearby capsules will not necessarily have their centers of mass in the same shear plane. For example, special care has to be taken in vesicle experiments to ensure that this is approximately the case. Accordingly, Lac & Barthès-Biesel (2008) also modeled the three-dimensional motion of two capsules positioned in

two different shear planes ($\Delta X_3^{(0)} \neq 0$). In this case, a sideways leapfrog motion occurs with a maximum trajectory displacement along both the x_2 - and x_3 - directions, which decreases as $\Delta X_3^{(0)}$ and/or capsule deformability increase. Lac and Barthès-Biesel also showed that the final trajectory shift along the x_3 -axis is indeed smaller than the one along the velocity gradient x_2 -axis (about one third), but present nevertheless. This was also globally confirmed by Gires *et al.* (2014) for vesicles.

However, in all aforementioned studies, the two capsules always had a significant initial relative velocity, obtained by means of $\Delta X_2^{(0)} \geq 0.5a$. This choice was made to avoid very long computations. The only exceptions are due to Lac *et al.* (2007) and Omori *et al.* (2013), who showed that for two capsules located on the same streamline ($\Delta X_1^{(0)} \neq 0, \Delta X_2^{(0)} = \Delta X_3^{(0)} = 0$), the perturbation created by the deformation and membrane rotation of the two capsules, created a small but finite velocity field that displaced the centroids along the x_2 -axis and led to a relative velocity of the capsules and to a leapfrog motion. The result was interesting as it showed that such initial conditions led to the largest self-diffusion effect. The conclusion of this review is that there is presently no information on the self-diffusion of two capsules when their centres are located in the x_1x_3 -plane.

The objective of this paper is to fill this gap and to investigate the three-dimensional motion of two capsules when their centroids are in or near the same x_1x_3 -plane. We will take advantage of the computational technique that we have developed, based on the coupling of a boundary integral to compute the flow and finite elements to compute the capsule wall mechanics (Walter *et al.* 2010). This coupling has proved to be very stable in a number of situations where long transient motion of a single capsule needed to be monitored (Walter *et al.* 2011; Hu *et al.* 2012; Dupont *et al.* 2013, 2016). We will see that a new interaction mode is revealed: given the choice, the capsules oscillate around the shear gradient axis, rather than around the vorticity axis. We call this interaction mode *the minuet motion*, as it is similar to the one reported for Volvox algae (Drescher *et al.* 2009), albeit for different hydrodynamic interactions.

The paper is organized as follows: the problem is set out in section 2 together with a short description of the numerical method. The different types of capsule interaction are presented in section 3, where we also discuss the main factors that determine the motion type. In section 4, we analyze which factors determine the motion type and illustrate the area of space where oscillatory motion is expected to occur. In section 5, we then study the consequences on the trajectory shift and self-diffusion phenomena in the suspension. In the final section 6, we summarize the findings and provide a conclusion.

2. Problem statement and numerical method

2.1. Problem description

Two identical spherical capsules C_1 and C_2 (radius a), filled with a Newtonian liquid (viscosity μ , density ρ) and enclosed by a very thin hyper-elastic membrane (surface shear modulus G_s and area dilation modulus K_s), are freely suspended in another Newtonian liquid (viscosity μ , density ρ) and subjected to a simple shear flow with shear rate $\dot{\gamma}$. Inertia effect is neglected. The capsules centroids are denoted G_1 and G_2 . We use a reference frame centered on G_1 , that moves with it (Figure 1). Our objective is to study the interaction process between the two capsules as they are convected by the flow and, specifically, to compute the evolution of the velocity $\mathbf{V}(t)$ and position $\mathbf{X}(t)$ of G_2 with time t .

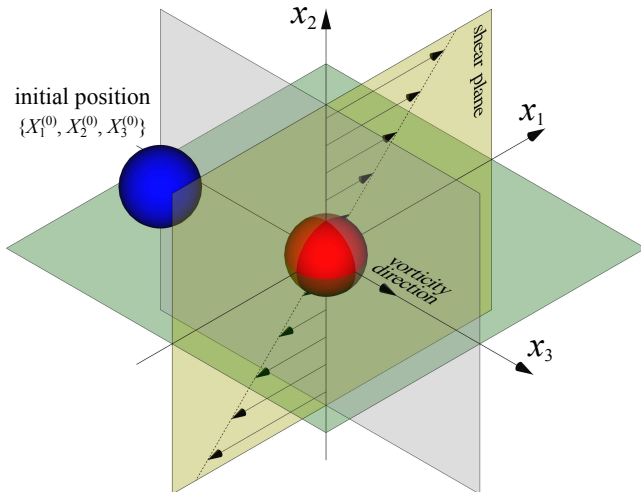


Figure 1: Two capsules flowing in simple shear flow. The reference frame is linked to capsule C_1 and the coordinate system is centered on it. The centre of C_2 is initially positioned at $\mathbf{X}^{(0)}$.

The undisturbed flow \mathbf{v}^∞ of the external liquid is given by:

$$\mathbf{v}_1^\infty(\mathbf{x}) = \dot{\gamma} x_2 \quad ; \quad v_2^\infty(\mathbf{x}) = v_3^\infty(\mathbf{x}) = 0. \quad (2.1)$$

Note that since the problem is inertialess, the flow field has the same expression (2.1) in a laboratory reference frame. The motion of the internal and external fluids is governed by the Stokes equations, with associated boundary conditions given by:

- vanishing flow perturbation far from the capsules:

$$\mathbf{v}^{ext}(\mathbf{x}) \rightarrow \mathbf{v}^\infty(\mathbf{x}) \quad \text{as} \quad \|\mathbf{x} - \mathbf{x}(G_\alpha)\| \rightarrow \infty \quad \alpha = 1, 2; \quad (2.2)$$

- at a material point \mathbf{x} located on the membrane of either capsule:

$$\mathbf{v}^{ext}(\mathbf{x}) = \mathbf{v}^{int}(\mathbf{x}) = \dot{\mathbf{x}}, \quad (2.3)$$

$$\mathbf{q} + \nabla_s \cdot \mathbf{T} = \mathbf{0}, \quad (2.4)$$

where the superscript *ext* or *int* refers respectively to the suspending fluid or to the capsule internal liquid. The jump of viscous traction across the membranes is \mathbf{q} , the in-plane elastic tension tensor in the membrane is denoted \mathbf{T} and ∇_s is the surface gradient operator. Equation (2.4) is the membrane equilibrium equation, which expresses the dynamic coupling between the solid membranes and the fluids.

As this fluid-structure interaction problem is now classical, we will only present the main hypotheses used here and refer the reader to the comprehensive review of Barthès-Biesel (2016). The fluid velocity at any point \mathbf{x} is written as a boundary integral on the surfaces S_1 and S_2 of the two capsules (Lac *et al.* 2007):

$$\mathbf{v}(\mathbf{x}) = \mathbf{v}^\infty(\mathbf{x}) - \frac{1}{8\pi\mu} \int_{S_1 \cup S_2} \mathbf{J}(\mathbf{x}, \mathbf{y}) \cdot \mathbf{q}(\mathbf{y}) dS(\mathbf{y}), \quad (2.5)$$

where \mathbf{J} is the free space Green's function given by:

$$\mathbf{J}(\mathbf{x}, \mathbf{y}) = \frac{\mathbf{I}}{\|\mathbf{x} - \mathbf{y}\|} + \frac{(\mathbf{x} - \mathbf{y}) \otimes (\mathbf{x} - \mathbf{y})}{\|\mathbf{x} - \mathbf{y}\|^3}, \quad (2.6)$$

where \mathbf{I} is the identity tensor. The pressure $p - p_0$ at a point \mathbf{x} is given by:

$$p(\mathbf{x}) - p_0 = -\frac{1}{4\pi} \int_{S_1 \cup S_2} \frac{\mathbf{q}(\mathbf{y}) \cdot (\mathbf{x} - \mathbf{y})}{\|\mathbf{x} - \mathbf{y}\|^3} dS(\mathbf{y}), \quad (2.7)$$

where p_0 denotes the far field pressure.

The capsule membrane is assumed to be an infinitely thin sheet of a three-dimensional isotropic volume incompressible material that satisfies a neo-Hookean (NH) constitutive law. Bending resistance is neglected. The membrane constitutive law relates the principal elastic tensions (forces per unit arclength measured in the membrane plane) T_1 and T_2 to the two principal extension ratios λ_1 and λ_2 :

$$T_1 = \frac{G_s}{\lambda_1 \lambda_2} \left[\lambda_1^2 - \frac{1}{(\lambda_1 \lambda_2)^2} \right], \quad (2.8)$$

with a similar expression for T_2 , where the subscripts 1 and 2 are permuted. For simplicity, we have denoted those principal directions 1 and 2, but they should not be confused with the Cartesian directions in space. The surface shear elastic modulus G_s and area dilation modulus K_s are related by $K_s = 3G_s$ (Barthès-Biesel 2016). The corresponding total deformation energy of the membrane of one capsule is given by:

$$W = \frac{G_s}{2} \int_S \left(\lambda_1^2 + \lambda_2^2 - 2 + \frac{1}{\lambda_1^2 \lambda_2^2 - 1} \right) dS, \quad (2.9)$$

where S stands for either S_1 or S_2 .

The main parameters are the capillary number:

$$Ca = \frac{\mu \dot{\gamma} a}{G_s}, \quad (2.10)$$

which measures the relative stiffness of the capsule and the initial position of G_2 at time $t = 0$, when the flow is suddenly started:

$$\mathbf{X}(0) = \mathbf{X}^{(0)} = \{X_1^{(0)}, X_2^{(0)}, X_3^{(0)}\}. \quad (2.11)$$

We shall discuss the typical case where $X_1^{(0)}$ and $X_3^{(0)}$ are negative while $X_2^{(0)}$ is positive: the flow of G_2 occurs from left to right in the trajectory figures. The case $X_3^{(0)} > 0$ is the symmetric of the typical case with respect to the shear plane. Positive values of $X_1^{(0)}$ and negative ones for $X_2^{(0)}$ correspond to the mirror image of the typical case, with respect to the $x_2 x_3$ -plane. When the crossing process is completed, the final steady position of G_2 is $\{X_1^{(f)}, X_2^{(f)}, X_3^{(f)}\}$. We define the final trajectory shifts of the capsule:

$$\delta_2 = |X_2^{(f)}| - |X_2^{(0)}|, \quad \delta_3 = |X_3^{(f)}| - |X_3^{(0)}|, \quad (2.12)$$

which are computed for $|X_1^{(f)}| = 10a$.

2.2. Numerical method

The fluid-structure interaction problem is solved by means of the numerical scheme that couples a boundary integral method (BI) to solve the fluid flow and the finite element method (FE) to solve the membrane mechanics (Walter *et al.* 2010; Hu *et al.* 2012). This method is well adapted to Stokes flows and has the advantage to request the discretization of the capsule surfaces S_1 and S_2 only. It automatically accounts for an unbounded fluid domain. The model inputs are the capillary number Ca and the initial position $\mathbf{X}^{(0)}$ of capsule C_2 . Following Lac *et al.* (2007), we use the fact that the two capsules are identical

to center the flow field on the midpoint O of G_1G_2 , so that Equation (2.5) can be solved on only one capsule and becomes:

$$\mathbf{v}(\mathbf{x}) = \mathbf{v}^\infty(\mathbf{x}) - \frac{1}{8\pi\mu} \int_{S_2} [\mathbf{J}(\mathbf{x}, \mathbf{y}) - \mathbf{J}(\mathbf{x}, -\mathbf{y})] \cdot \mathbf{q}(\mathbf{y}) dS(\mathbf{y}), \quad (2.13)$$

The capsule surface S_2 is discretized using P_2 triangle elements, in which 6 nodes are allocated at the vertices and the middle of each sides. The mesh is generated from the initial spherical shape by projecting a regular icosahedron to the sphere and then subdividing each element subsequently to the desired precision. A mesh of 1280 elements and 2562 nodes has been used in all the simulations, corresponding to a characteristic mesh size $\Delta h_c = O(0.1a)$. Such a spatial discretization has been shown to lead to a relative error of order 10^{-3} on the Taylor deformation of a single capsule in shear flow (Walter *et al.* 2010). Furthermore, it can withstand some membrane compression without creating any numerical instability (Hu *et al.* 2012). The explicit time iteration will be stable only if the time step is such that $\dot{\gamma}\Delta t < O(Ca\Delta h_c/a)$ (Walter *et al.* 2010). In the case of an NH membrane and $Ca = 0.3$, $\dot{\gamma}\Delta t = 5 \times 10^{-4}$ allows us to compute the capsule trajectory over long times without stability issues. We stop the computation when the distance G_1G_2 is larger than $10a$.

At time $t = 0$, C_2 (positioned at $\{X_1^{(0)}/2, X_2^{(0)}/2, X_3^{(0)}/2\}$) and C_1 (positioned at $\{-X_1^{(0)}/2, -X_2^{(0)}/2, -X_3^{(0)}/2\}$) are subjected to the sudden start of the flow. The model follows the motion of the capsule membrane over time. At any time, the model can thus output the position of the surface nodes, from which it is possible to infer, for each capsule, the deformation and elastic tensions in the membrane as well as the position and velocity of the centroid. The knowledge of this velocity allows us to transcript the results in the reference frame linked to C_1 .

The accuracy of the numerical model is checked by comparing capsules trajectories with those obtained by Lac *et al.* (2007) and Lac & Barthès-Biesel (2008), and also by assessing the influence of the time step and of the spatial discretization of the capsule membranes (Appendix A): the conclusion is that the centroid trajectories are accurate within $0.05a$.

3. Types of capsule interaction: simple crossing (leapfrog) or minuet motion

A major finding of our work is that, depending on the initial position of C_2 , there are two types of motion:

- Simple crossing (also denoted leapfrog): C_2 catches up with C_1 , interacts and goes away. The two capsules are not necessarily in the same shear plane.
- Minuet motion: C_2 catches up with C_1 , interacts, overpasses C_1 , reverses its motion and repeats the process one, two or three times before getting away.

The two motions are illustrated and analyzed in the following.

3.1. Single interaction: leapfrog motion

As a reference, we consider the situation where the two capsules are in the shear plane on the same streamline ($X_1^{(0)} = 10a, X_2^{(0)} = 0, X_3^{(0)} = 0, Ca = 0.3$). Similar computations have been made by Lac *et al.* (2007) for pre-inflated capsules, but only the value of the final trajectory shift is reported. Under Stokes flow conditions, the capsules must remain in this plane. The trajectory of C_2 is shown in Figures 2a,b (Movie 1).

When the flow is started, the two capsules are far enough from each other, that they

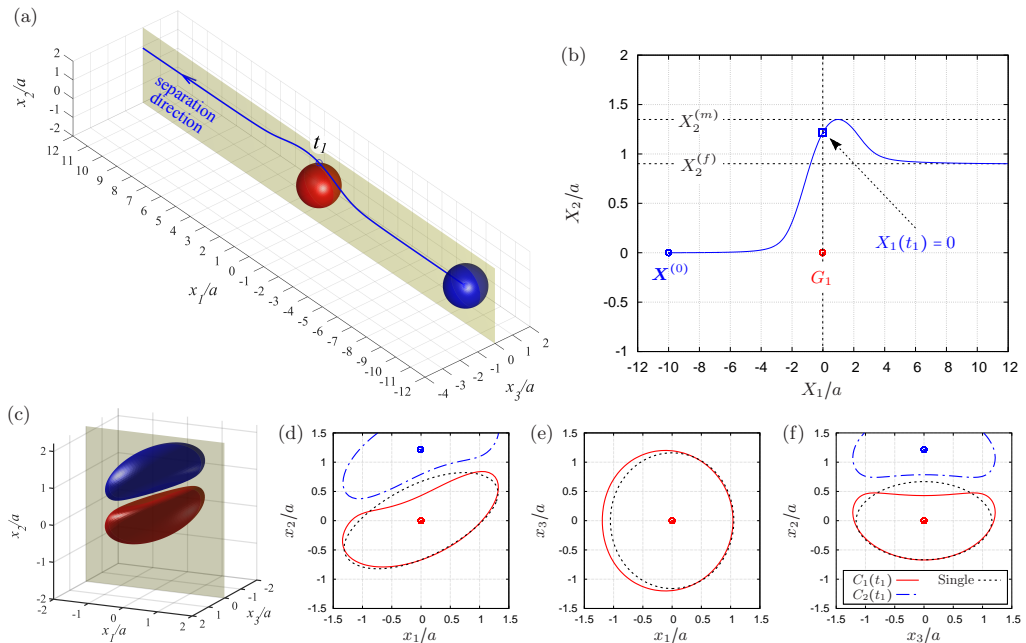


Figure 2: Leapfrog motion of two capsules with their centres in the same shear plane ($X_1^{(0)}/a = -10$, $X_2^{(0)} = 0$, $X_3^{(0)} = 0$, $Ca = 0.3$). (a) Three-dimensional view of the trajectory of C_2 . (b) G_2 trajectory in the shear plane. (c) Three-dimensional view of the deformed capsules at t_1 when $X_1(t_1) = 0$. (d, e, f) C_1 intersections with the three coordinates planes at t_1 .

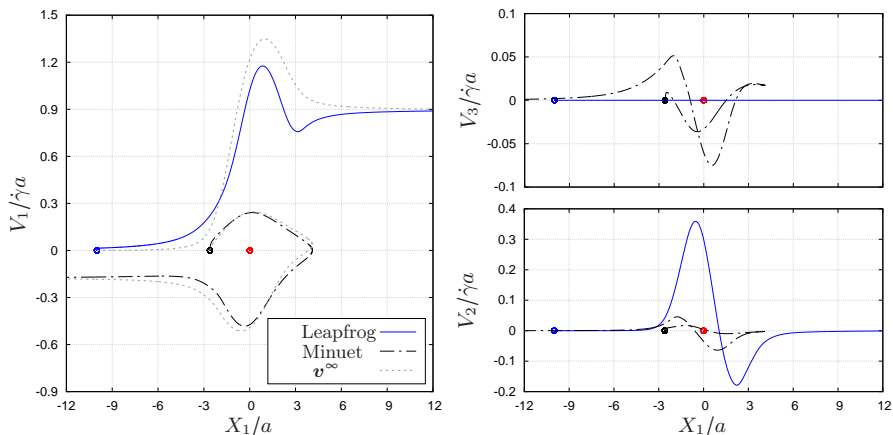


Figure 3: Evolution of C_2 velocity during a leapfrog ($X_1^{(0)}/a = -10$, $X_2^{(0)} = X_3^{(0)} = 0$) or minuet ($X_1^{(0)}/a = X_3^{(0)}/a = -2.6$, $X_2^{(0)} = 0$) for $Ca = 0.3$.

behave as if they were almost alone in the fluid. Within $\dot{\gamma}t \sim 6$ they reach a roughly ellipsoidal shape around which the membrane rotates, as shown in Figure 2d (see the review by Barthès-Biesel (2016)). The deformation and rotation of C_1 lead to a stresslet that creates a small velocity field and a small depression. This perturbation displaces C_2 along the velocity gradient in the direction that moves it *towards* C_1 , as shown in

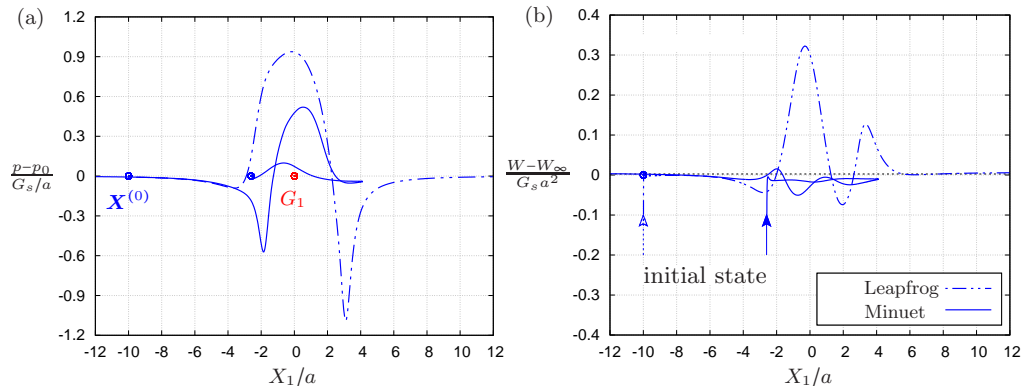


Figure 4: Pressure and membrane energy evolution during the leapfrog and minuet motions for $Ca = 0.3$. (a) Pressure p at the mid-point between G_1 and G_2 ; (b) membrane elastic energy W . Leapfrog: $X_1^{(0)}/a = -10$, $X_2^{(0)} = 0$, $X_3^{(0)} = 0$. Minuet: $X_1^{(0)}/a = -2.6$, $X_2^{(0)} = 0$, $X_3^{(0)}/a = -2.6$.

Figure 2b. Note that this phenomenon is the opposite of the one observed by Doddi & Bagchi (2008) when inertia is taken into account. As a consequence, $V_2(t) > 0$ for $t > 0$ and C_2 is convected towards C_1 , as shown in Figures 2a,b. The only way for C_2 to overpass C_1 is to ‘jump’ over it in the x_1x_2 -plane (thus the term ‘leapfrog motion’). The fact that the motion is constrained to the shear plane leads to a high velocity difference $\|\mathbf{V} - \mathbf{v}^\infty\|/\dot{\gamma}a$ in the x_1 - and x_2 - directions (Figure 3). The evolution of the pressure at the mid point between G_1 and G_2 (Equation 2.7) can also explain the interaction phenomenon: indeed, as $|X_1(t)/a|$ decreases, the pressure in the lubrication film between the two capsules increases (Figure 4a) and pushes C_2 in the x_2 -direction, along which the maximum displacement of G_2 is $X_2^{(m)}$. As C_2 overpasses C_1 , the widening of the lubrication film leads to a depression (Figure 4a), which decreases X_2 , until a final steady value $X_2^{(f)}$ is reached when the two capsules are far apart ($|X_1| \geq 6a$, in this case). The final trajectory shift $\delta_2 = |X_2^{(f)} - X_2^{(0)}|$ is $0.9a$, and is equal to the one found by Lac *et al.* under the same flow situation for a 5% pre-inflation. The finite value of δ_2 indicates that the two capsule interaction leads to self-diffusion effects in a dilute suspension of capsules. The deformed profiles of C_1 (equivalently of C_2) in the x_1x_2 -, x_1x_3 - and x_2x_3 -planes are shown in Figures 2d, e, f at time $\dot{\gamma}t_1 = 9.7$, when the two capsules cross, which we define by $X_1(t_1) = 0$. Figures 2d, f show that there is indeed a thin lubrication film between the two capsules (which corroborates the pressure build-up) and that the two capsules are highly deformed. The global deformation can be assessed through the membrane elastic energy W given by Equation (2.9). The value of $W(X_1) - W_\infty$, where W_∞ is the deformation energy of a single capsule, allows us to estimate the intensity of the mechanical interaction between the two capsules. During the close interaction, the two capsules undergo large transient deformation, leading to a peak in $W - W_\infty$ (Figure 4b). The separation process leads to some deformation oscillations, until a final steady state is reached, which is identical to the single capsule one, elastic energy wise (Figure 4b).

3.2. Minuet motion

We now consider the case $X_1^{(0)}/a = -2.6$, $X_2^{(0)} = 0$, $X_3^{(0)}/a = -2.6$, $Ca = 0.3$, where capsule C_2 is located *off* the shear plane and can thus move freely in space: this leads

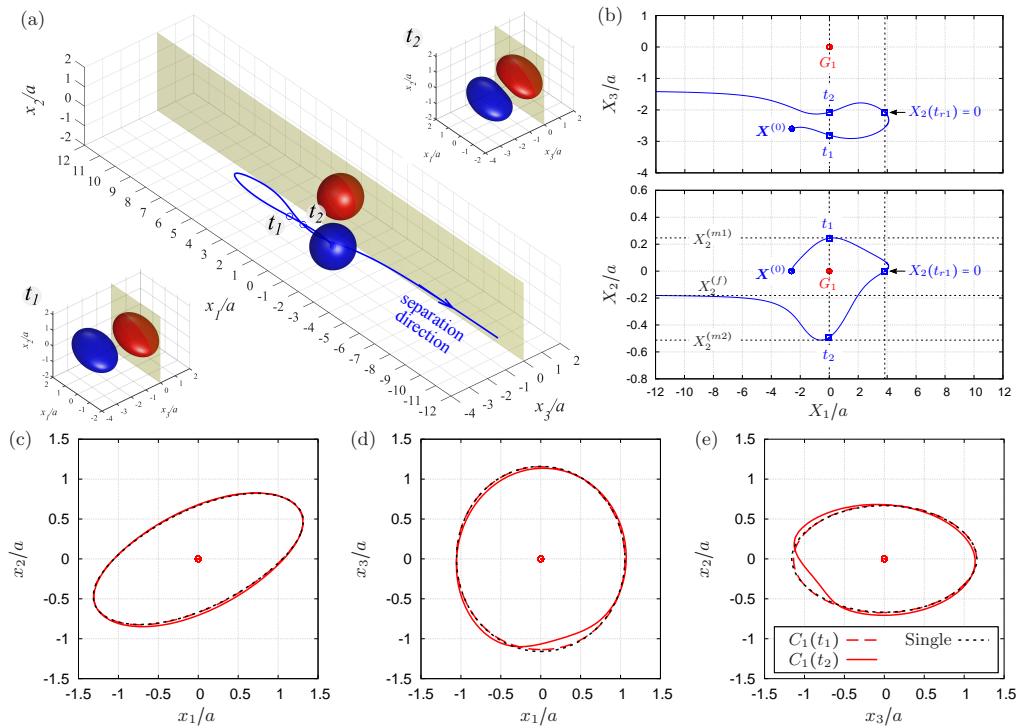


Figure 5: Minuet of two capsules ($X_1^{(0)}/a = -2.6$, $X_2^{(0)} = 0$, $X_3^{(0)}/a = -2.6$, $Ca = 0.3$). (a) Three-dimensional view of the trajectory of C_2 . (b) Projections of G_2 trajectories in the x_1x_2 - and x_1x_3 -planes. (c, d, e) C_1 profile intersections with the three coordinates planes at times t_1 and t_2 when $X_1(t_1) = X_1(t_2) = 0$.

to trajectories that are completely different from the ones described above. As in the previous case, the rotation of C_1 displaces G_2 along the velocity gradient, so that C_2 is convected towards C_1 . The three-dimensional trajectory of C_2 is shown in Figure 5a, where the two capsules are shown in their initial position (Movie 2). In order to get a clearer grasp of the process, we analyse the trajectories of the projections of G_2 in the x_1x_2 - and x_1x_3 -planes in Figure 5b. As $|X_1(t)/a|$ decreases, the pressure increases slightly (Figure 4a): this leads to a slight increase in both $|X_2(t)|$ and $|X_3(t)|$ (Figure 5b), which allows enough space for capsule C_2 to overpass C_1 by moving *around* the x_2 -axis (insert in Figure 5a). Correspondingly, the maximum displacement $|X_2^{(m1)}|$ is smaller than in the leapfrog situation. Similarly, the velocity difference $\|\mathbf{V} - \mathbf{v}^\infty\|/\dot{\gamma}a$ remains small while occurring in all three directions as shown in Figure 3. The energy variation $W - W_\infty$ is also very small (Figure 4b), which indicates that there is little mechanical interaction between the capsules. This point is further corroborated by the quasi superposition of the deformed profiles of C_1 at time t_1 when $X_1(t_1) = 0$, and when it is alone in the flow (Figures 5c, d, e).

As the capsules separate, the small depression (Figure 4a) leads to a negative displacement along the x_2 -axis, which takes G_2 into the reverse flow region and entices C_2 to move back towards C_1 . The pressure is still negative when the reversal takes place, so that $|X_3(t)|$ decreases. As a consequence, there is not enough space for C_2 to move around C_1 in a x_1x_3 -plane and a sideways leapfrog motion takes place, which is qualitatively similar to the one that occurs in the shear plane, as described in the previous section: there is

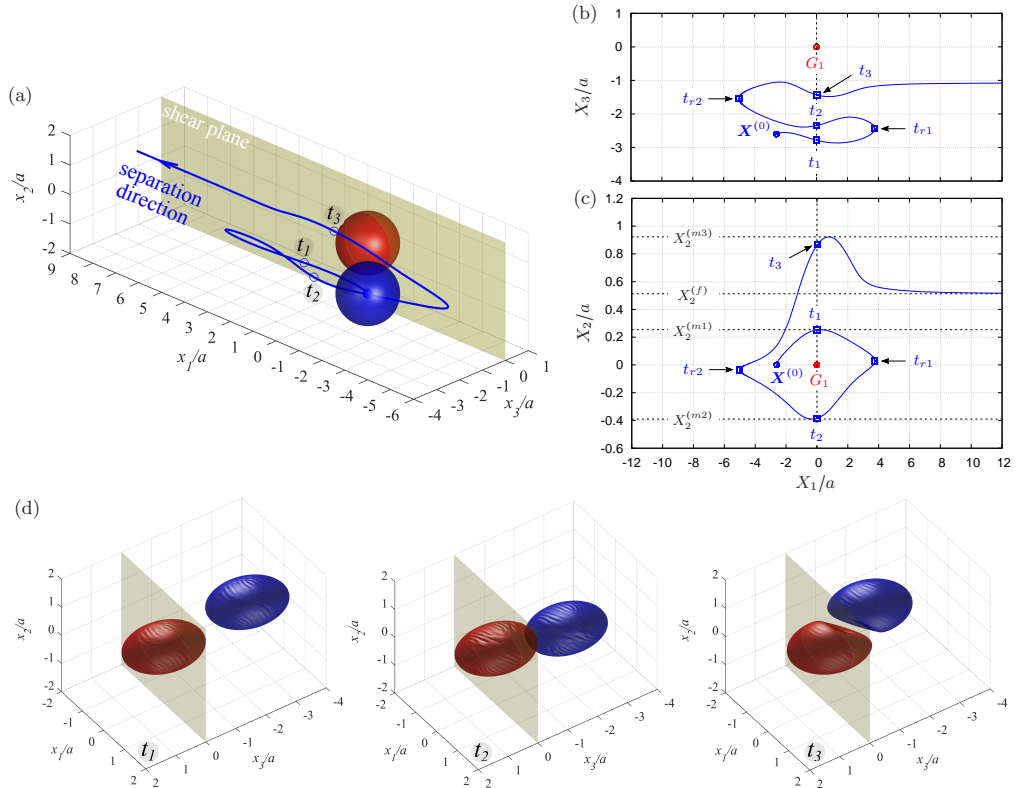


Figure 6: Minuet with multiple reversals for $X_1^{(0)}/a = -2.6$, $X_2^{(0)} = 0$, $X_3^{(0)}/a = -2.6$, $Ca = 0.2$. The instants of close interaction when $X_1 = 0$ are denoted t_1 , t_2 and t_3 in chronological order. (a) Three-dimensional view of the trajectory of C_2 . (b, c) Projections of G_2 trajectories in the x_1x_2 - and x_1x_3 -planes. (d) Three-dimensional profiles at close interaction.

a significant pressure build-up in the lubrication film, followed by a depression as the capsules part (Figure 4a). The pressure variation leads to an increase of $|X_2(t)|$ up to a value $|X_2^{(m2)}|$, which is large enough to allow the further decrease to the final displacement $|X_2^{(f2)}|$, without crossing into a reverse flow region. At time t_2 when $X_1(t_2) = 0$, the two capsules are closer than at time t_1 and thus undergo a transient deformation as appears in Figure 5a (insert) and in Figures 5d, e. Correspondingly, the mechanical energy $W - W_\infty$ undergoes a transient variation, which, however, is much smaller than the one that occurs when the capsules cross in the shear plane (Figure 4b). We deduce that minuet motion is less energy consuming than leapfrog motion.

If we now start with the same initial conditions ($X_1^{(0)}/a = -2.6$, $X_2^{(0)} = 0$, $X_3^{(0)}/a = -2.6$) but reduce the capsule deformability by setting $Ca = 0.2$, two reversals occur, as shown in Figure 6 (Movie 3 and Movie 4). The first reversal is essentially the same as for $Ca = 0.3$. However, when the capsules cross again at time t_2 , there is still enough space to allow crossing around the x_3 -axis. Furthermore, the displacement along the x_2 -axis is still small ($X_2(t_2)/a = -0.39$), compared to the one observed for $Ca = 0.3$ ($X_2(t_2)/a = -0.51$), so that the pressure induced trajectory shift forces G_2 to cross again into the reverse flow region: the capsule is thus convected again towards C_1 . During the third crossing,

since $|X_3(t_3)|/a < 2$, the capsule has to do a sideways leapfrog motion that leads to a displacement $X_2(t_2)/a = 0.92$, that is large enough to accommodate the trajectory shift without changing the flow direction of the capsule: the latter finally goes back in the direction where it came from. Note that at time t_3 , the two capsules undergo a significant transient deformation, due to a strong interaction. This phenomenon is unexpected in view of the fairly large initial distance between the capsules.

4. What factors determine the motion type?

The type of motion (leapfrog or minuet) is determined by the evolution of $X_2(t)$ after crossing, since it is a change of sign of $X_2(t)$ that causes reversal of motion. At crossing, the film pressure displaces G_2 along the velocity gradient, to a maximum value $|X_2^{(m)}|$. After crossing, the separation process and the subsequent depression lead to a displacement Δ_2 of G_2 back to the x_1 -axis. For leapfrog motion, the trajectory shift is easily identified as $\Delta_2 = |X_2^{(m)} - X_2^{(f)}|$ (see Figure 2b). When reversal occurs, the film pressure decrease also leads to a trajectory shift Δ_2 , which is difficult to evaluate in a simple fashion. However, since Δ_2 is a consequence of the separation process, we can surmise that it follows an evolution similar to the one found in leapfrog motion in the shear plane, i.e. that it decreases when the capsule separation $|X_2^{(0)}|$ and/or $|X_3^{(0)}|$ increase and when the capsule deformability Ca increases (Lac *et al.* 2007; Lac & Barthès-Biesel 2008; Pranay *et al.* 2010; Omori *et al.* 2013; Gires *et al.* 2014). We conclude that whenever $|X_2^{(m)}|$ is less than Δ_2 , reverse motion is to be expected. The main parameters that determine the values of $|X_2^{(m)}|$ and of Δ_2 , are the initial capsule separation $\mathbf{X}^{(0)}$ and the capillary number Ca . We now study their influence separately.

4.1. Effect of the initial capsule separation $\mathbf{X}^{(0)}$

The effect of the initial offset $|X_3^{(0)}|$ from the shear plane is shown for $Ca = 0.3$, $X_1^{(0)}/a = -3.0$ and $X_2^{(0)}/a = 0$ in Figure 7. When $|X_3^{(0)}|$ is small (e.g., $|X_3^{(0)}/a| \leq 2$), the situation is close to the one when the two capsules are in the same shear plane. Correspondingly, they undergo a sideways leapfrog motion with a displacement $|X_2^{(m)}/a| \geq 0.4$, which is large enough to allow direct crossing (Figure 7a). For a larger offset $|X_3^{(0)}/a| \geq 2.6$, C_2 has room to move around C_1 in a x_1x_3 -plane: then the displacement $|X_2^{(m)}/a| \sim 0.2$ is small (Figure 7a), and thus reversal motion occurs during separation. As $|X_3^{(0)}|$ increases, the influence of C_1 decreases and the two capsules have almost no relative velocity. The motion shown in Figure 7 for $|X_3^{(0)}/a| = 4$ is near the limit of what can be reasonably computed: indeed the capsule reaches $X_1 = 0$ at time $\dot{\gamma}t_1 = 50$ at the first crossing, and at time $\dot{\gamma}t_2 = 266$ at the second crossing. We conclude that the minuet motion is slow.

We now turn to the effect of the initial distance $|X_1^{(0)}|$ on the trajectory of C_2 , as shown in Figure 8 for $Ca = 0.3$, $X_2^{(0)}/a = 0$ and $X_3^{(0)}/a = -2.6$. Note that since $|X_3^{(0)}/a| > 2$, C_2 has room to move around C_1 in a x_1x_3 -plane. However, the far field perturbation created by C_1 is a stresslet, which varies as the square of the inverse distance G_1G_2 . It is this perturbation that displaces G_2 along the x_2 -axis and gives C_2 the small relative approach velocity, which leads to crossing. This perturbation velocity varies as $[X_1^{(0)}/a]^{-2}$ when $|X_1^{(0)}/a| \gg 1$ ($|X_1^{(0)}/a| > 4$ in this particular case). Even though it is small, its prolonged effect over a long time leads to a significant $|X_2^{(m)}|$ displacement and thus to a sideways leapfrog motion. Note that the initial position $X_2^{(0)}/a = 0$ is unstable when the capsules

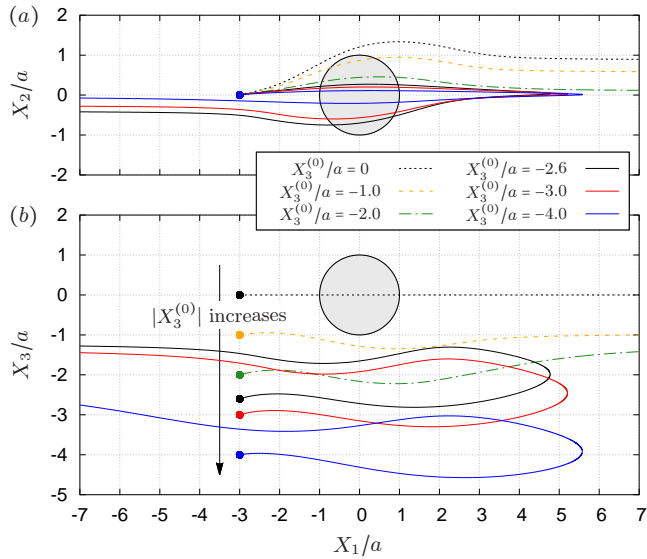


Figure 7: Effect of the initial position $X_3^{(0)}$ on the capsule trajectory for $Ca = 0.3$, $X_1^{(0)}/a = -3.0$ and $X_2^{(0)}/a = 0$. Projections of G_2 trajectories in the x_1x_2 -plane (a) and in the x_1x_3 -plane (b). When $|X_3^{(0)}/a| \leq 2$, capsule C_2 has not enough room to move around C_1 : it overpasses it with a sideways leapfrog motion.

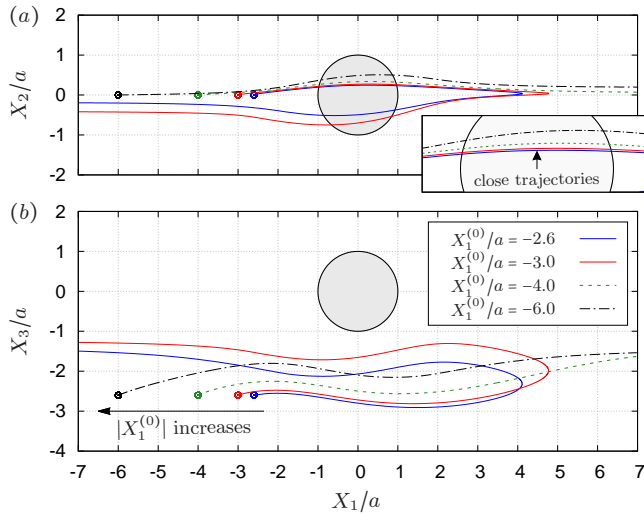


Figure 8: Effect of the initial position $X_1^{(0)}$ on the capsule trajectory for $Ca = 0.3$, $X_2^{(0)}/a = 0$ and $X_3^{(0)}/a = -2.6$. Projections of G_2 trajectories in the x_1x_2 -plane (a) and in the x_1x_3 -plane (b). When $|X_1^{(0)}/a| \geq 4$, capsule C_2 has sufficiently moved across streamlines that it can overpass C_1 with a sideways leapfrog motion.

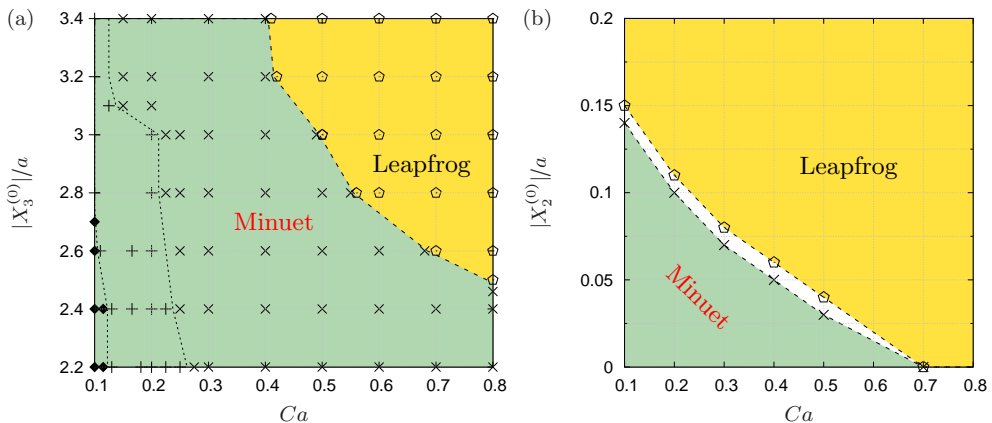


Figure 9: Phase diagrams for motion type: (a) Motion type as function of Ca and $X_3^{(0)}$ for $X_1^{(0)} = X_3^{(0)}$ and $X_2^{(0)} = 0$. The points represent the positions of G_2 at rest: \times one oscillation, $+$ two oscillations, \blacklozenge three oscillations. (b) Motion type as a function of Ca and $X_2^{(0)}$ for $|X_1^{(0)}|/a = |X_3^{(0)}|/a = 2.6$.

interact. However, when the initial distance $|X_1^{(0)}|$ becomes of order a (e.g., $|X_1^{(0)}|/a = 3$), the displacement $|X_2^{(m)}|$ has no time to build up and remains small: then reversal occurs.

Similar situations of capsule interaction have been considered by Lac & Barthès-Biesel (2008), who did not report any motion reversal, even when they studied three-dimensional motions with non zero values of $X_3^{(0)}$. This is due to the fact that they started with $X_2^{(0)}/a \geq 0.5$ and $X_1^{(0)}/a \geq 10$, values which were too large for minuet to occur.

4.2. Effect of capsule deformability

Under given flow conditions, the capsule deformability is accounted for by the capillary number Ca and increases with it. Some global results are presented under the form of phase diagrams. For $X_2^{(0)} = 0$ and $|X_1^{(0)}| = |X_3^{(0)}|$, the effect of varying the initial capsule separation and deformability is shown in Figure 9a. Minuet thus occurs roughly for $2 < |X_3^{(0)}|/a < 4$. For $|X_3^{(0)}|/a > 4 \sim 5$, the capsule separation is so large that the relative velocity is very small and the capsule doublet configuration remains essentially stationary. The effect of Ca is complex: for a typical separation $|X_3^{(0)}|/a = 2.6$ and up to $Ca \leq 0.7$, a minuet takes place with one reversal for moderate values of deformability ($0.2 < Ca < 0.7$) or two (or more) reversals when $Ca \leq 0.2$. This transition from one to two reversals when Ca is reduced has been illustrated in section 3.2. However, for large capsule deformability ($Ca > 0.7$), no motion reversal occurs: the capsules are so deformed and tilted towards the flow direction, that, when they overpass, their trajectory perturbation is small. The effect of $X_2^{(0)}$ is shown in Figure 9b for the typical case $|X_1^{(0)}|/a = |X_3^{(0)}|/a = 2.6$. Minuet occurs only for small values of $|X_2^{(0)}|/a$ and moderate Ca , i.e., for small relative velocities between two capsules with moderate deformability. This limited range of minuet motion explains why it had not been detected before.

Note that the inherent deformability of a capsule even when Ca is very small, makes it different from a rigid sphere. Consequently, it is impossible to find permanent capsule doublets like those predicted by Batchelor & Green (1972b) for two spheres freely suspended in simple shear flow: indeed such doublets can occur only for perfect spheres as pointed out by the authors.

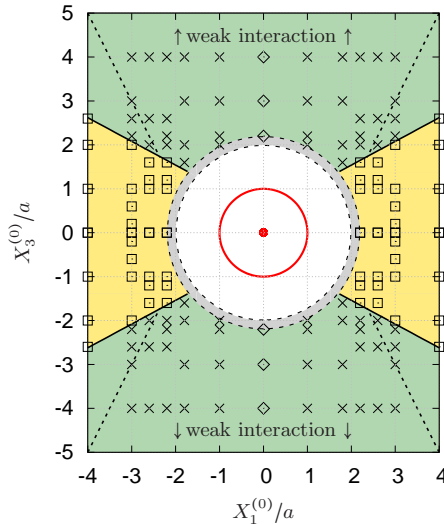


Figure 10: Domain of doublet formation around capsule C_1 for $X_2^{(0)} = 0$, $Ca = 0.3$ and a NH membrane. The sphere of radius $2a$ is a steric exclusion area, while the grey zone between the spheres of radii $2.2a$ and $2a$ is an exclusion region, that leaves a space $0.2a$ between the two capsules. The points represent the positions of G_2 at rest, and the symbols indicate the motion type: \times minuet, \square leapfrog, \diamond steady doublet. The position of the boundary between the two domains for $Ca = 0.5$ is indicated by a dash line.

4.3. Region of minuet motion

The domain around C_1 , where long term doublets are formed is illustrated in Figure 10 for $Ca = 0.3$. The sphere of radius $2.2a$ centered on G_1 is an exclusion region, that leaves a space $0.2a$ between the two capsules. When $X_1^{(0)} = X_2^{(0)} = 0$, the capsule doublet separated by $X_3^{(0)}$, remains stationary. Whenever the centre of capsule C_2 is located in the yellow area, the two capsules will cross once (leapfrog motion) and separate. In the green area, the two capsules will remain close and oscillate a few times before eventually separating. For $|X_3^{(0)}|/a \gtrsim 4$, the interaction becomes weak, so that the doublet configuration remains essentially stationary. The minuet domain shown in Figure 10 is in fact three-dimensional and extends in the x_2 -direction over a small distance of order $0.06a$ for $Ca = 0.3$ (see Figure 9b). When Ca is decreased the boundary between leapfrog and minuet motions does not change appreciatively, but the thickness of the three-dimensional minuet domain increases. Conversely as shown in Figure 10, when Ca increases, the boundary is tilted towards the x_3 -axis and the minuet domain thickness decreases. Note that for $X_2^{(0)} \geq 0.5a$, the whole region would be yellow (apart from the exclusion area).

An important consequence of the minuet motion is linked to the fact that it tends to push together two capsules that were initially distant and not expected to interact much. This point is illustrated in Figure 6 where the initial separation $G_1G_2 - 2a = 1.7a$ is decreased during crossing to a film with thickness roughly $0.2a$, which is thin enough to lead to potential physicochemical interactions or damage.

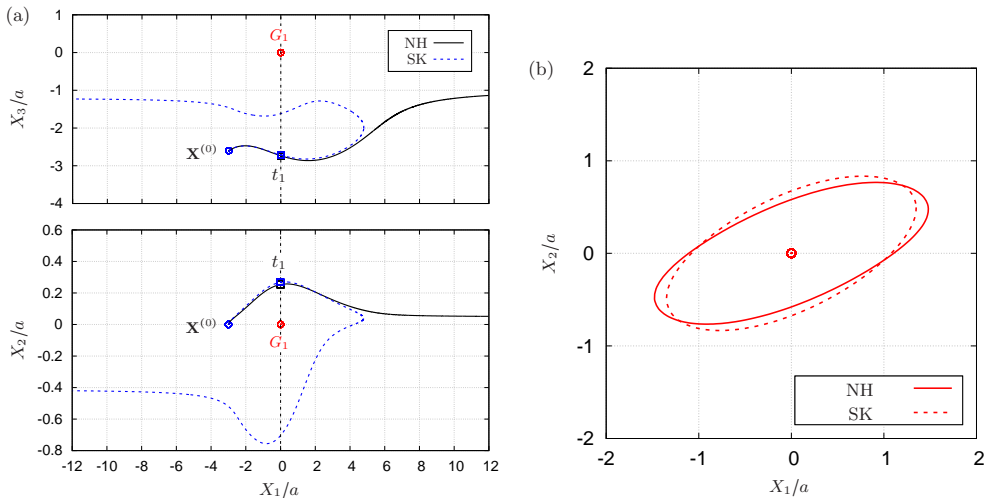


Figure 11: Interaction process of two capsules with a NH membrane or a SK membrane for $Ca = 0.5$, $X_1^{(0)}/a = -3$, $X_2^{(0)} = 0$, $X_3^{(0)}/a = -2.6$. (a) The NH capsule does a sideways leapfrog motion, while the SK capsule does a motion reversal. (b) Deformed profiles of the capsule C_1 at time t_1 defined by $X_1(t_1) = 0$.

4.4. Effect of the membrane constitutive equation

It is of interest to assess the influence of the wall constitutive law, as all the above results have been obtained for a neo-Hookean (NH) membrane. In particular, it is possible to assume that the principal tensions and elongations are related by the Skalak law (SK) (Skalak *et al.* 1973), which reads:

$$T_1 = \frac{G_s}{\lambda_1 \lambda_2} \left[\lambda_1^2 (\lambda_1^2 - 1) + C (\lambda_1 \lambda_2)^2 [(\lambda_1 \lambda_2)^2 - 1] \right]. \quad (4.1)$$

The surface shear elastic modulus is G_s and the area dilation modulus is given by $K_s = (1 + 2C)G_s$. The two laws (2.8) and (4.1) predict the same small deformation behavior for $C = 1$, but for large deformations, the NH law is strain-softening, whereas SK law is strain-hardening (Barthès-Biesel *et al.* 2002). Correspondingly, for the same value of Ca , the deformation of a single capsule in simple shear flow is larger for a NH membrane than for a SK one (Barthès-Biesel 2016).

We can then expect that the transition between a leapfrog and a minuet motion will happen for values of Ca that will be different for capsules with SK or NH membranes. In order to verify this prediction, we model the interaction of two capsules enclosed either by an SK membrane ($C = 1$) or an NH membrane, in the case $X_1^{(0)}/a = -3.0$, $X_2^{(0)} = 0$, $X_3^{(0)}/a = -2.6$ and $Ca = 0.5$. As shown in Figure 11a, the NH capsules do a sideways leapfrog motion whereas the SK capsules undergo one oscillation and reverse their direction of motion. The explanation to this difference of behavior is linked to the fact that the NH capsule is more deformed than the SK one (Figure 11b), and that its trajectory displacement Δ_2 is thus small enough to prevent it from going into the reverse flow region.

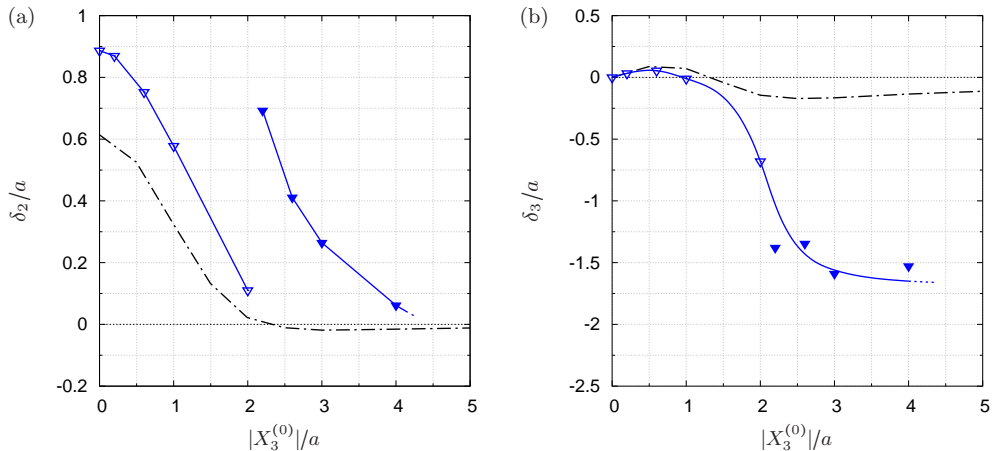


Figure 12: Irreversible trajectory shifts δ_2 and δ_3 , computed at $|X_1^{(f)}|/a = 10$, as a function of $X_3^{(0)}$ ($X_1^{(0)}/a = -3.0$, $X_2^{(0)} = 0$, $Ca = 0.3$). Open symbols correspond to leapfrog motion, filled ones to minuet motion. The dash-dot line corresponds to the results of Lac & Barthès-Biesel (2008), obtained for $X_1^{(0)}/a = -10$, $X_2^{(0)}/a = 0.5$ and $\beta = 1.05$.

5. Global effects: trajectory shift and doublet duration

5.1. Trajectory shift

When two capsules with a NH membrane are in the same shear plane ($X_3^{(0)}/a = 0$), it is a well established fact that after crossing, the two capsules are irreversibly displaced from their initial trajectory: for a given value of Ca , the trajectory shift $\delta_2 = |X_2^{(f)}| - |X_2^{(0)}|$ is maximum for $X_2^{(0)}/a = 0$, decreases when $|X_2^{(0)}|$ increases and becomes almost zero for $|X_2^{(0)}/a > 2$ (Lac & Barthès-Biesel 2008; Pranay *et al.* 2010; Omori *et al.* 2013; Gires *et al.* 2014). The effect of $X_3^{(0)}/a$ is mostly reported for the case $X_2^{(0)}/a = 0.5$: then δ_2 is maximum for $X_3^{(0)}/a = 0$, decreases to almost zero for $|X_3^{(0)}/a \geq 2$ (Lac & Barthès-Biesel 2008; Gires *et al.* 2014). The trajectory shift along the vorticity direction $\delta_3 = |X_3^{(f)}| - |X_3^{(0)}|$ is small and less than $0.1a$ (see also Figure 15). The effect of Ca is small and does not change the findings. The influence of the membrane constitutive law on the leapfrog motion in the shear plane was studied by Pranay *et al.* (2010), who compared the effect of a NH or SK law ($C = 10$) on the trajectory shift δ_2 . They found that for the same Ca , δ_2 is larger for an SK law than for an NH one: this is due to the high apparent rigidity of the SK law, linked to a high value of the area dilation modulus.

The new results for $X_2^{(0)}/a = 0$ are illustrated for $Ca = 0.3$ in Figure 12, where they are compared with the results of Lac & Barthès-Biesel (2008), obtained for $X_2^{(0)}/a = 0.5$. For $X_3^{(0)}/a \leq 2$ when a leapfrog motion occurs, the shift δ_2 decreases with $X_3^{(0)}/a$ and is about 50% larger for $X_2^{(0)}/a = 0$ than for $X_2^{(0)}/a = 0.5$ (Figure 12a): this is in agreement with the previously reported evolution of δ_2 with $X_2^{(0)}/a$ and $X_3^{(0)}/a$. However, when the doublet motion evolves from leapfrog to minuet, a bifurcation takes place for $|X_3^{(0)}/a = 2.1 \pm 0.1$: δ_2 jumps to values that are about one order of magnitude larger than the ones that would be expected from the previous $X_2^{(0)}/a = 0.5$ results or from the prolongation of the leapfrog curve for δ_2 .

Similarly, whereas the shift δ_3/a remains small during the leapfrog motion, it becomes

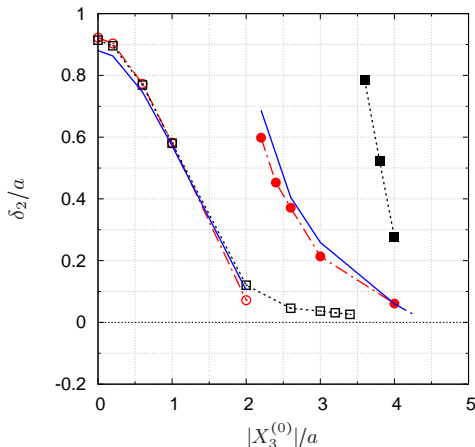


Figure 13: Trajectory shift δ_2 as a function of $X_3^{(0)}$ for different membranes constitutive laws ($X_1^{(0)}/a = -3.0$, $X_2^{(0)} = 0$). The solid line corresponds to a neo-Hookean membrane with $Ca = 0.3$ (Figure 12). The dashed lines correspond to a Skalak membrane ($C=1$); \circ $Ca = 0.5$, \square $Ca = 1.0$. Open symbols: leapfrog motion; filled symbols: minuet motion.

large and negative for $X_2^{(0)}/a \geq 2$ (Figure 12b). This means that at the end of the interaction process, the capsule C_2 is nearer the shear plane x_1x_2 , than when the flow started. The minuet motion thus leads to a shift δ_3 along the vorticity direction, which tends to reduce the initial distance between the two capsules, in opposition to a diffusive effect. But since the capsule separation in the x_3 -direction is reduced, a sideways leapfrog motion takes place, with a resulting large value of δ_2 , and thus diffusive effects along the shear gradient direction. Decreasing Ca does not change much the above results. However, when the capsule deformability increases, the bifurcation occurs for increasingly large values of $|X_3^{(0)}/a$ and is difficult to compute as the minuet becomes very slow (see section 5.2).

The influence of the membrane law is shown in Figure 13: the SK capsule undergoes a leapfrog motion for $|X_3^{(0)}/a \leq 2$ and then makes a minuet for $|X_3^{(0)}/a \geq 2.2$. The evolutions of δ_2 are almost superimposed for an NH membrane ($Ca = 0.3$) and for an SK membrane ($Ca = 0.5$). When the SK capsule deformability increases to $Ca = 1.0$, the transition between leapfrog and minuet motions occurs further away, around $|X_3^{(0)}/a \sim 3.5$. We can then conclude that, indeed, the effect of a strain-hardening membrane would just be to shift the results to larger values of Ca , without changing the essence of the interaction process.

5.2. Doublet duration

The minuet motion, when it occurs, is very slow as shown in Figure 14 for $X_1^{(0)}/a = -3.0$ and $X_2^{(0)}/a = 0$. The time $\hat{\gamma}t_1$ at which the first crossing occurs, increases with the separation $|X_3^{(0)}/a$, but does not depend on Ca , the membrane law or the ulterior type of motion (leapfrog or minuet). The fact that $\hat{\gamma}t_1$ increases with $|X_3^{(0)}/a$ is due to the fact that the relative velocity of C_2 , which is initially zero, builds up from a flow perturbation (due to C_1), the intensity of which decreases with the square of the distance between the two capsules. The time $\hat{\gamma}t_2$ of the second crossing is quite large and increases significantly with capsule deformability and distance.

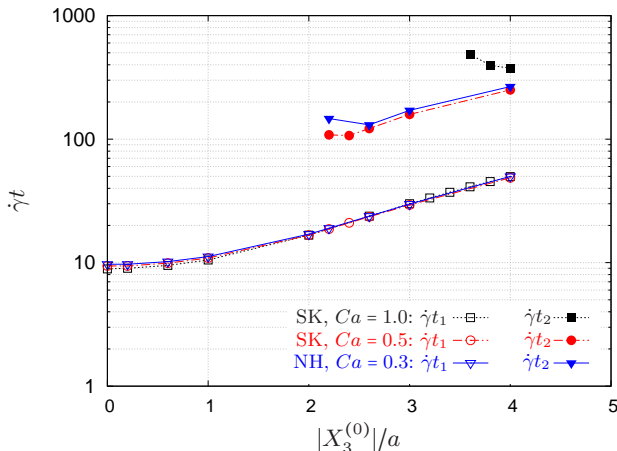


Figure 14: Effect of Ca , $X_3^{(0)}$ and constitutive law on the times $\dot{\gamma}t_1$ and $\dot{\gamma}t_2$ of first and second crossings ($X_1^{(0)}/a = -3.0$ and $X_2^{(0)}/a = 0$).

This means that the two capsules remain close to each other for a long time, while drifting slowly. When $|X_3^{(0)}|/a \geq 4$, $\dot{\gamma}t_2$ becomes too large to be reliably computed (the values of $\dot{\gamma}t_2$ for $Ca = 1.0$ and an SK membrane are very high, and are just here to illustrate the phenomenon).

6. Discussion and conclusion

The situation that we have studied pertains to a semi-dilute suspension of capsules that is suddenly put in motion by a simple shear flow. The novel aspect of our work is that we consider a pair of nearby capsules with their centres in (or near) the plane normal to the velocity gradient ($X_2^{(0)} \sim 0$). This capsule configuration had never been studied before, because it entails long computations. Indeed, the only results on capsule interaction off the shear plane had been obtained for capsules with a significant relative velocity, which prevented minuet from occurring and which led to weak capsule interactions and small trajectory displacement.

When $X_2^{(0)} \sim 0$, the important results are:

- The capsule pair can remain stable for a long time, while dancing a minuet.
- When they separate, the capsules can reverse direction.
- When one or more oscillations occur, the irreversible trajectory shift is large.
- This minuet dance progressively brings the capsules to closely interact and deform significantly.
- The less deformable the capsule, the more prone it is to do a minuet.
- The zone where a minuet can occur has been identified.

During the close interaction, the film thickness between the two capsules is of the order of $\sim 0.1a - 0.2a$. For small capsules, this may lead to physico-chemical interaction.

In order to make the problem consistent, we considered as initial condition a suspension of spherical capsules at rest, and suddenly started the flow. When the capsules are pre-deformed to the profile that they would have if they were alone in the flow, we have verified that they take the same motion (leapfrog or minuet) as if they were initially spherical: the only difference is that, for pre-deformed capsules, the first close interaction happens $\dot{\gamma}t \leq 5$ earlier than for spherical capsules. It follows that the minuet interaction is

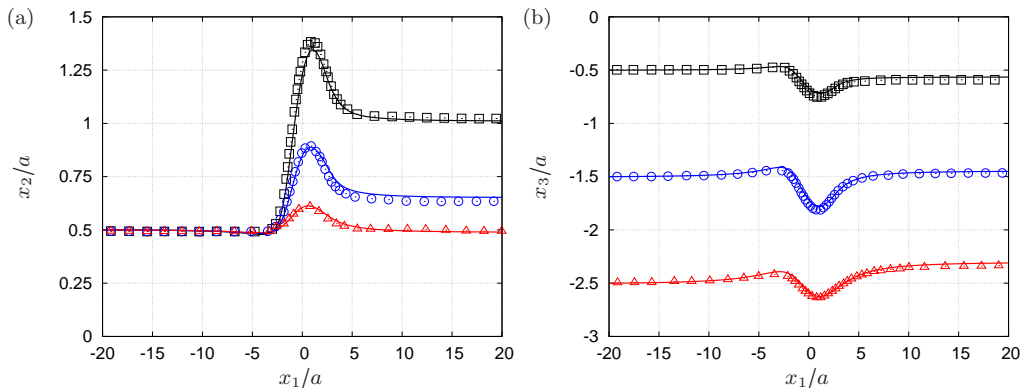


Figure 15: Projection of G_2 trajectories for $\beta = 1.05$, $Ca = 0.45$ and different initial positions. Capsule C_2 starts from $X_1^{(0)}/a = -20$, $X_2^{(0)}/a = 0.5$ and different $X_3^{(0)}$. The comparison between the results of Lac & Barthès-Biesel (symbols) and the present results (lines) shows very good agreement.

not restricted to the transient start of the flow of a suspension. For example, from Figure 6, we note that at the end of the interaction, when C_2 is located at $X_1/a = 5.0$, $X_2/a = 0.54$, $X_3/a = -1.1$, it has almost recovered its equilibrium shape. Suppose that C_2 then meets a new capsule C_3 , located in the vicinity of $X_1/a = 7.6$, $X_2/a = 0.54$, $X_3/a = 1.5$. Being in the same relative configuration as C_1 and C_2 were at time $t = 0$, capsules C_2 and C_3 will do a minuet. We can thus expect minuet motions in semi-dilute suspensions.

In conclusion, we have shown a novel and unexpected effect in the pair interaction of two capsules, that depends on the relative position of the two particles. It would be interesting to check experimentally the existence of long lasting capsule doublets that do a minuet motion.

Acknowledgments

This work was supported by the European Research Council (ERC) Consolidator grant (MultiphysMicroCaps, No. 772191), by the National Natural Science Foundation of China (No. 11402084) and by the China Scholarship Council (Visiting Scholar Scholarship of X.-Q. Hu).

Declaration of Interests: the authors report no conflict of interest.

Appendix A

The results of the BI-FE model (1280 elements) are first compared to those obtained by Lac *et al.* (2007) and Lac & Barthès-Biesel (2008) for two pre-inflated capsules with an NH membrane and radius βa , where β is the inflation ratio. The pre-stress is created by means of an internal pressure p_0 , which leads to an isotropic elastic tension $T_0 = p_0 a/2$, given by Laplace's law. For a neo-Hookean membrane, $T_0 = 6G_s(\beta - 1)$ in the limit of small inflation. The trajectories of G_2 obtained with the two methods show very good agreement, as illustrated in Figure 15 for $Ca = 0.45$.

As the minuet motion is a novel phenomenon, which occurs over fairly long times, it is of importance to verify that the trajectories do not suffer from error accumulation over time. The test case consists of two capsules enclosed by an SK membrane ($C = 1$) with $Ca = 0.5$, $X_1^{(0)}/a = -3.0$, $X_2^{(0)} = 0$ and $X_3^{(0)}/a = -2.4$. As shown in Figure 13,

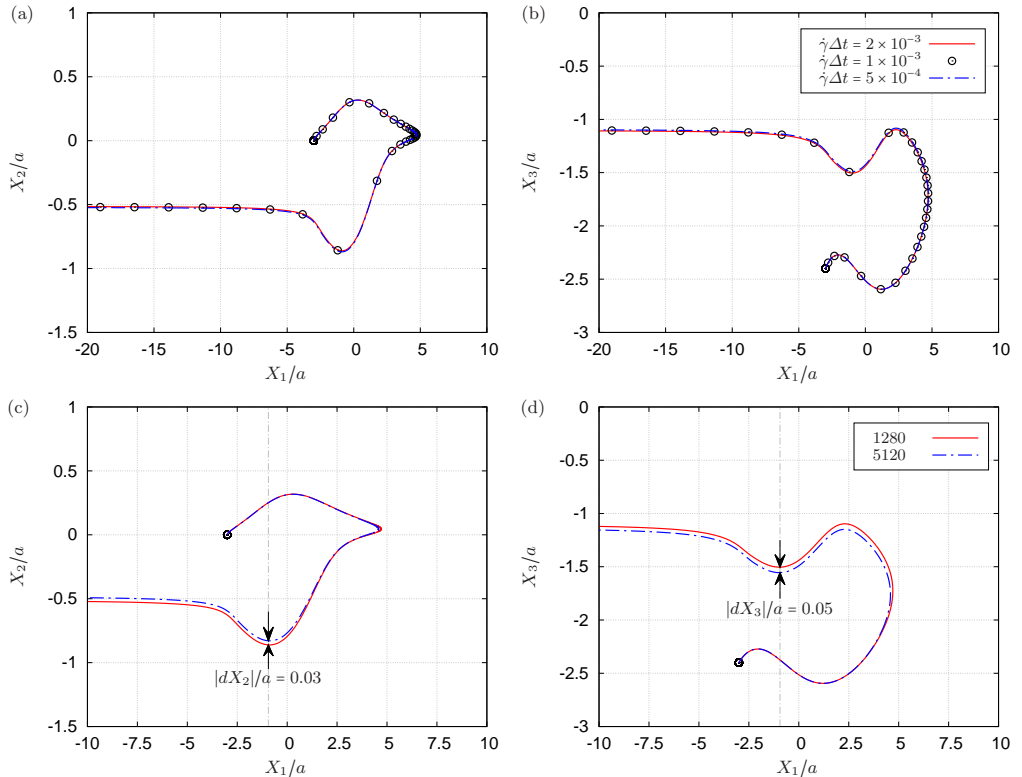


Figure 16: Effect of numerical parameters on the G_2 trajectory, projected on the x_1x_2 - and x_1x_3 -planes for SK membranes, for $Ca = 0.5$, $X_1^{(0)}/a = -3.0$, $X_2^{(0)}/a = 0$, $X_3^{(0)}/a = -2.4$. (a, b) Effect of time step for 1280 elements. (c, d) Effect of mesh refinement for $\dot{\gamma}\Delta t = 2 \times 10^{-3}$.

those capsules undergo a minuet with one reversal. The choice of an SK law rather than an NH one enables us to use larger values of Ca , and thus larger time steps for similar trajectories. As shown in Figure 16a for 1280 elements on the capsule surfaces, decreasing the time step $\dot{\gamma}\Delta t$ from 2×10^{-3} to 5×10^{-4} has no effect on the trajectory. Conversely, we keep the same time step $\dot{\gamma}\Delta t = 2 \times 10^{-3}$ and compare the trajectories obtained with two spatial meshes with 1280 or 5120 elements, corresponding to mesh sizes $\Delta h_c = O(0.1a)$ and $O(0.05a)$, respectively. As shown in Figure 16b, the trajectories differ by at most one (fine) mesh size at the interaction point. We conclude that the trajectories, that are presented in this study using 1280 elements and $\dot{\gamma}\Delta t = 5 \times 10^{-4}$, are reliable and that the final trajectory shifts δ_2/a and δ_3/a have an error of the order of 0.05a.

REFERENCES

- BARTHÈS-BIESEL, D. 2016 Motion and deformation of elastic capsules and vesicles in flow. *Annual Review of Fluid Mechanics* **48** (1), 25–52.
- BARTHÈS-BIESEL, D., DIAZ, A. & DHENIN, E. 2002 Effect of constitutive laws for two dimensional membranes on flow-induced capsule deformation. *Journal of Fluid Mechanics* **460**, 211–222.
- BATCHELOR, G. K. & GREEN, J. T. 1972a The determination of the bulk stress in a suspension of spherical particles to order c^2 . *Journal of Fluid Mechanics* **56** (2), 401–427.

- BATCHELOR, G. K. & GREEN, J. T. 1972*b* The hydrodynamic interaction of two small freely-moving spheres in a linear flow field. *Journal of Fluid Mechanics* **56** (2), 375–400.
- DODDI, S. K. & BAGCHI, P. 2008 Effect of inertia on the hydrodynamic interaction between two liquid capsules in simple shear flow. *International Journal of Multiphase Flow* **34** (4), 375–392.
- DRESCHER, K., LEPTOS, K. C., TUVAL, I., ISHIKAWA, T., PEDLEY, T. J. & GOLDSTEIN, R.E. 2009 Dancing Volvox: hydrodynamic bound states of swimming algae. *Phys. Rev. Lett.* **102**, 168101.
- DUPONT, C., DELAHAYE, F., BARTHÈS-BIESEL, D. & SALSAC, A.-V. 2016 Stable equilibrium configurations of an oblate capsule in simple shear flow. *Journal of Fluid Mechanics* **791**, 738–757.
- DUPONT, C., SALSAC, A.-V. & BARTHÈS-BIESEL, D. 2013 Off-plane motion of a prolate capsule in shear flow. *Journal of Fluid Mechanics* **721**, 180–198.
- GIRES, P. Y., SRIVASTAV, A., MISBAH, C., PODGORSKI, T. & COUPIER, G. 2014 Pairwise hydrodynamic interactions and diffusion in a vesicle suspension. *Physics of Fluids* **26** (1), 013304.
- GUAZZELLI, E. & MORRIS, J. F. 2012 *A physical introduction to suspension dynamics*. Cambridge University Press.
- GUIDO, S. & SIMEONE, M. 1998 Binary collision of drops in simple shear flow by computer-assisted video optical microscopy. *Journal of Fluid Mechanics* **357**, 1–20.
- HU, X.-Q., SALSAC, A.-V. & BARTHÈS-BIESEL, D. 2012 Flow of a spherical capsule in a pore with circular or square cross-section. *Journal of Fluid Mechanics* **705**, 176–194.
- KANTSLEER, V., SEGRE, E. & STEINBERG, V. 2008 Dynamics of interacting vesicles and rheology of vesicle suspension in shear flow. *EPL* **82** (1), 58005.
- LAC, E. & BARTHÈS-BIESEL, D. 2008 Pairwise interaction of capsules in simple shear flow: Three-dimensional effects. *Physics of Fluids* **20** (4), 040801.
- LAC, E., MOREL, A. & BARTHÈS-BIESEL, D. 2007 Hydrodynamic interaction between two identical capsules in simple shear flow. *Journal of Fluid Mechanics* **573**, 149–169.
- LOEWENBERG, M. & HINCH, E. J. 1997 Collision of two deformable drops in shear flow. *Journal of Fluid Mechanics* **338**, 299–315.
- OLAPADE, P. O., SINGH, R. K. & SARKAR, K. 2009 Pairwise interactions between deformable drops in free shear at finite inertia. *Physics of Fluids* **21** (6), 063302.
- OMORI, T., ISHIKAWA, T., IMAI, Y. & YAMAGUCHI, T. 2013 Shear-induced diffusion of red blood cells in a semi-dilute suspension. *Journal of Fluid Mechanics* **724**, 154–174.
- PRANAY, P., ANEKAL, S. G., HERNANDEZ-ORTIZ, J. P. & GRAHAM, M. D. 2010 Pair collisions of fluid-filled elastic capsules in shear flow: Effects of membrane properties and polymer additives. *Physics of Fluids* **22** (12), 123103.
- SINGH, R. K. & SARKAR, K. 2015 Hydrodynamic interactions between pairs of capsules and drops in a simple shear: Effects of viscosity ratio and heterogeneous collision. *Physical Review E* **92** (6), 063029.
- SKALAK, R., TOZEREN, A., ZARDA, R. P. & CHIEN, S. 1973 Strain energy function of red blood cell membranes. *Biophysical Journal* **13**, 245–264.
- WALTER, J., SALSAC, A.-V. & BARTHÈS-BIESEL, D. 2011 Ellipsoidal capsules in simple shear flow: prolate versus oblate initial shapes. *Journal of Fluid Mechanics* **676**, 318–347.
- WALTER, J., SALSAC, A.-V., BARTHÈS-BIESEL, D. & LE TALLEC, P. 2010 Coupling of finite element and boundary integral methods for a capsule in a Stokes flow. *International Journal for Numerical Methods in Engineering* **83** (7), 829–850.